Electronic energy transfer at semiconductor interfaces. I. Energy transfer from two dimensional molecular films to Si(111)

A. P. Alivisatos, M. F. Arndt, S. Efrima, D. H. Waldeck, and C. B. Harris

Citation: The Journal of Chemical Physics **86**, 6540 (1987); doi: 10.1063/1.452396
View online: http://dx.doi.org/10.1063/1.452396
View Table of Contents: http://scitation.aip.org/content/aip/journal/jcp/86/11?ver=pdfcov
Published by the AIP Publishing

Electronic energy transfer at semiconductor interfaces. I. Energy transfer from two-dimensional molecular films to Si(111)

A. P. Alivisatos,[a] M. F. Arndt, S. Efrima,[b] D. H. Waldeck,[c] and C. B. Harris[d]
Department of Chemistry and Materials and Molecular Research, Division of Lawrence Berkeley Laboratory, University of California, Berkeley, California 94720

(Received 22 September 1986; accepted 24 February 1987)

The fluorescence decays from submonolayers of pyrene separated from Si(111) by Xe spacer layers are measured as a function of spacer thickness (17–200 Å), pyrene coverage, and emission wavelength. The results are explained in terms of two decay channels: energy transfer and trapping among the molecules in the two-dimensional pyrene overlayer, and excitation of electrons from the valence to the conduction band in the Si(111) by the dipole near field of the electronically excited pyrene molecule. The intralayer energy transfer is modeled using the Kohlrausch equation $N(t) = N_0 \exp(-t/\tau)^{\alpha}$, in which α is related to the distribution of pyrene molecules in energy. Energy transfer from the molecule to the semiconductor is modeled using the classical image dipole theory. The classical model is used to calculate the energy transfer rates from a dipole to Si and GaAs as a function of dipole–semiconductor separation, and as a function of dipole emission wavelength.

I. INTRODUCTION

Little is known about the photophysical properties of electronically excited molecules on the surface of a semiconductor, despite their importance to a number of diverse fields, including photoetching[1] and solar energy conversion.[2] The electronically excited molecule at the semiconductor surface usually decays orders of magnitude faster than the isolated molecule. The mechanisms responsible for this can be classified into two groups: those in which the semiconductor acts as a support, and energy transfer events among the highly concentrated molecules in the adsorbed overlayer determine the decay time;[3] and those in which the electronic and optical properties of the semiconductor perturb the excited molecule.[4–7]

The excitation energy in a disordered photoexcited overlayer can be rapidly transferred to a dimer or multimer which acts as a trap. For bulk materials, the classic theoretical approach to dynamical problems of this type is to start with a perfectly ordered solid, and then introduce a degree of disorder.[8] It is now possible to study excitation transfer and trapping in submonolayer films.[3,9–25] These studies afford the opportunity to approach the problem of energy transfer in disordered solids from a different perspective. By varying the coverage of such a thin film, the evolution from an isolated molecule to a bulk solid can be studied. In this paper, some ideas which have proven useful in the study of excitation transfer and trapping in bulk amorphous solids will be applied to disordered submonolayers of molecules near semiconductor surfaces.

In addition to acting as a support, the semiconductor itself can act as a trap for the excitation energy of the two-dimensional molecular layer. If the molecular emission energy exceeds the semiconductor band gap the molecule can nonradiatively excite an electron from the valence band to the conduction band in the semiconductor by a dipole–induced dipole mechanism, analogous to Förster energy transfer between two molecules or to energy transfer between a molecule and a metal.[4–7] This energy transfer process is predicted to increase in efficiency with the inverse molecule–semiconductor separation cubed, and can lead to a reduction in the lifetime and quantum yield of four to six orders of magnitude (compared to the dilute solution lifetime) when the molecule is a few angstroms from the surface. Despite the importance of this effect it has not received much attention, so that even coarse estimates of the energy transfer rates from molecules to semiconductors are not available. One method for studying this type of energy transfer is to measure the lifetime of the molecular emission as a function of separation from the solid, employing spacer layers to fix the distance.[7]

In this paper, the results will be presented from a spacer layer experiment in which the molecular emission energy exceeds the semiconductor band gap. The fluorescence decays of pyrene separated from a silicon substrate by xenon spacer layers are measured as a function of spacer thickness, pyrene coverage, and emission wavelength. An indirect band gap material was chosen as the energy acceptor because it does not absorb visible energy as strongly as a direct gap material, like GaAs, and consequently the energy transfer rate to the surface, although very fast, will be comparatively slower, permitting measurements at smaller molecule–semiconductor separations.

It is sensible to choose a molecule for these experiments with a very large absorption cross section, in the neighborhood of 50 000 ℓ/mol cm and with a near unity fluorescence quantum yield, so the signal level will be observable even when the molecule is close to the surface. The lifetime of the molecular excited state must also be relatively long compared to that of most singlet states, so that there will be

[a] Present address: AT&T Bell Labs, 600 Mountain Ave., Murray Hill, NJ 07974.
[b] Permanent address: Department of Chemistry, Ben Gurion University of the Negev, Beer Shiva, Israel 84105.
[c] Permanent address: Department of Chemistry, University of Pittsburgh, Pittsburgh, PA 15260.
[d] To whom correspondence should be addressed.

 0021-9606/87/116540-10$02.10

sufficient time resolution at small molecule–semiconductor separations. These two sets of requirements are contradictory, but can be reconciled by exciting a state which rapidly internally converts to another, longer-lived state. Pyrene fulfills these requirements[26] since it can be excited into S_2 with 335 nm light with an ϵ of 35 000 ℓ/mol cm, and efficiently internally converts to the S_1 state, which has a radiative rate of about $10^6\ s^{-1}$.

It what follows, the problem of excitation transfer and trapping in a molecular overlayer is discussed. Next, predictions for the energy transfer rate from molecules to semiconductors, computed using the classical model of Chance, Prock, and Silbey,[35] are presented. These calculations display trends as a function of molecular emission energy and separation from the semiconductor which, in the absence of extensive experimental information, are useful as a guide in thinking about this problem. The experimental procedure, and the results follow. In the final section the observed dynamics is discussed in terms of the two energy transfer processes.

II. THEORY

A. Models of two-dimensional energy transfer

The dynamics of photoexcited overlayers have been previously studied using both low[3,9–13] and high[14–25] surface area nonabsorbing substrates (band gap greater than the molecular emission energy). At coverages below a monolayer the fluorescence decays from such assemblies are nonexponential, which has been attributed to Förster energy transfer and trapping. Even though the number of molecules in such an experiment is small, they are highly concentrated. An upper limit on the average distance between molecules of 100 Å^2 area at one-tenth monolayer coverage is 30 Å, which is comparable to the Förster R_0 for a typical singlet transition.[27] At such high surface densities the molecules can stack, forming nonradiative dimers and multimers which act as traps. Consequently, the excitation energy can transfer between molecules in the layer until it finds a trap. In all of these experiments the fluorescence decay "rate" is found to increase with increasing coverage, as such a model would predict.

Many procedures have been proposed for modeling the dynamics within a two-dimensional amorphous photoexcited overlayer; Table I shows some of the proposed decay laws. These models make assumptions concerning the number of donors and acceptors and their radial and angular distribution functions. Then, assuming a mechanism for energy transfer (such as Förster or exchange), the exact decay function can be obtained. In Table I, Eqs. (2), (3), (4), and (6) are all decay laws of this type which have been applied to photoexcited monolayers. In addition, Baumann and Fayer have derived the decay functions corresponding to many other types of distributions.[34]

A common feature to the models presented above is that an averaging of the energy transfer rate takes place over the spatial distribution of the molecules. Alternatively, Richert,[32] and Richert and Bässler[33] have investigated the case

TABLE I. Decay law parameters.

Eq. (1). Biexponential
$N(t) = A_1 \exp(-t/\tau_1) + A_2 \exp(-t/\tau_2)$
$\langle\tau\rangle = (A_1\tau_1^2 + A_2\tau_2^2)/(A_1\tau_1 + A_2\tau_2)$ $\langle\tau\rangle$—expectation value of the time

Eq. (2). Förster energy transfer and trapping, one donor, one acceptor, isotropically distributed[a]
$N(t) = A \exp[-t/\tau - 1.354C(t/\tau)^{0.33}]$ τ—isolated molecule decay time
C—concentration of traps

Eq. (3). Förster energy transfer and trapping, one donor, one acceptor, one independent species, isotropically distributed[a]
$N(t) = A_1 \exp(-t/\tau_1) + A_2 \exp[-t/\tau_2 - 1.354C(t/\tau_2)^{0.33}]$

Eq. (4). Förster energy transfer and trapping, two donors, two acceptors, isotropically distributed, one independent species[b]
$N(t) = A_1 \exp(-t/\tau_1) + A_2 \exp[-t/\tau_2 - 1.354C_2(t/\tau_2)^{0.33}] + (1 - A_1 - A_2)\exp[-t/\tau_3 - 1.354C_3(t/\tau_3)^{0.33}]$

Eq. (5). Kohlrausch decay function[c]
$N(t) = A \exp(-t/\tau)^{\alpha}$ $0 < \alpha < 1$

Eq. (6). Förster energy transfer and trapping, one donor, one acceptor, distributed on a fractal surface[d]
$N(t) = A \exp[-C(t/\tau)^{\alpha} - t/\tau]$ C—concentration of traps
$0 < \alpha < 0.5$ τ—isolated molecule decay time
$\alpha = \hat{d}/s$ $\hat{d}$—fractal dimension
$s = 6$ for Förster energy transfer

Eq. (7). Förster energy transfer and trapping, Gaussian distribution of donor energies, distributed uniformly on a regular lattice[e]
$N(t) = A \exp[-C(t/\tau)^{\alpha} - t/\tau_0]$ C—concentration of traps
$0 < \alpha < 1$ τ—hopping time
$\alpha^{-1} = (\sigma/4kT)^2 + 1$ σ—inhomogeneous width
τ_0—isolated molecule decay time

[a] References 3 and 10.
[b] Reference 3.
[c] References 28–30.
[d] References 23–25 and 31.
[e] References 32 and 33.

in which there is excitation transfer and trapping among molecules located on a regular three-dimensional lattice, but whose energies are distributed according to a Gaussian distribution. If kT is less than the width of the Gaussian there will be a cascade from higher to lower energy as time progresses. High energy excitations can transfer their energy to lower energy ones, with the energy difference taken up by the surrounding bath. The low energy excitations cannot transfer their energy back without thermal activation. This means the high energy side of the spectrum will decay faster. According to such a model, the fluorescence decay will be given by an expression of the Kohlrausch type,[28–30] Eq. (5) in Table I, with an independent multiplicative decay time corresponding to isolated molecule decay, Eq. (7). The Kohlrausch equation models a system relaxing with a distribution of exponential decay times. The parameters defining this distribution are α, which is related to the width, and τ, the peak value. Richert and Bässler have applied this formalism to the dynamics of triplet excitons in bulk amorphous organic crystals with some success.[32,33] For these triplet states the exchange interaction, rather than Förster transfer, is the mechanism for the excitation transfer.

B. Molecule–semiconductor energy transfer

To date, two experiments have been performed on energy transfer from a molecule to a semiconductor, with contradictory results. Hayashi, Castner, and Boyd[6] measured the relative luminescence intensity from a 50 Å thick film of tetracene as a function of distance to Si and GaAs, and found that the quantum yield did not decrease below 100 Å. On the other hand, our group measured the lifetime of the first triplet state of pyrazine as a function of separation from GaAs, and showed that the lifetime monotonically decreases with decreasing separation, in a manner which approximately follows the $1/d^3$ law.[4] In a third experiment, Crackle and Struve[13] measured energy transfer rates from Cresyl Violet to TiO_2. In that experiment, the molecular emission energy is below the semiconductor band gap, and only the radiative rate of the molecule is effected by the semiconductor. In the absence of definite experimental information, it is useful to consider theoretical predictions of the energy transfer rates.

The classical model of Chance, Prock, and Silbey (CPS) has been successful in predicting the rates of energy transfer from molecules to metal surfaces.[7,35] Briefly, the CPS model assumes the electronically excited molecule is a classical oscillating point dipole; the solid is modeled as a semi-infinite continuous medium characterized by an optical dielectric constant, and separated from the spacer layer by a sharp boundary. The dipole field incident on the solid is partially reflected and partially absorbed in a manner governed by the dielectric constant. The incident and reflected fields, appropriately summed, give the value of the electric field at the dipole, in the presence of the solid. The imaginary part of the electric field at the dipole can then be related to the lifetime of the molecule. Application of the CPS model to energy transfer from molecules to semiconductors can be readily accomplished by substitution of the appropriate dielectric constant for the solid.

The rates of energy transfer from a molecule to Si and GaAs have been calculated using the CPS model,[35] as described previously.[7] Figure 1 shows the geometry used in the calculations. The molecule was assumed to have unity quantum yield and an isolated decay rate of 1. The dipole was imbedded in a spacer layer with the dielectric constant of argon,[36] 1.66. The spacer layer fixed the distance d from the molecule to the substrate. The dielectric constants for Si and GaAs measured by Aspnes and Studna[37] were employed in these calculations. Calculations were performed at 0.1 eV intervals for dipole energies between 1.5 and 4.0 eV. At each dipole emission energy, the energy transfer rate was calculated at 78 different distances ranging from 2 to 1000 Å.

At distances greater than 50–100 Å, the lifetime oscillates with distance and emission energy due to the modulation of the radiative rate of the molecule by the reflected field from the surface. There is no net absorption of energy by the solid, but depending on the wavelength and distance, the reflected field from the semiconductor with either be in or out of phase with the dipole, and hence will either damp or drive it. At distances below 50–100 Å, the lifetime is sharply reduced due to nonradiative energy transfer from the dipole near field. In this regime the lifetime varies with distance as $1/d^3$, and the variation of the lifetime with wavelength depends on the net absorption of the energy by the Si. Shown in Fig. 2 is a log–log plot of the energy transfer rate vs distance for one emission energy, 3.2 eV, for both Si and GaAs. At the shortest distance, 2 Å, the energy transfer rate is approximately 50 000 times greater than the isolated molecule radiative rate. In Fig. 3 the energy transfer rate is plotted vs emission energy, for the molecule located 10 Å away from the Si. The sharp increase in energy transfer rate at 3.4 eV is due to the onset of the direct interband absorption in Si.

Figures 2 and 3 can be used to estimate the classical prediction for the lifetime of the molecule for emission energies throughout the visible at distances where the $1/d^3$ term dominates. Since a quantum yield and an isolated molecular emission rate of unity were used, the energy transfer rate at 3.2 eV can be estimated for a molecule at this emission energy by multiplying the transfer rate in Fig. 2 for the appropriate distance by the molecular radiative rate. The wavelength can be scaled using Fig. 3. Figure 2 shows that the energy transfer rates to GaAs are about an order of magnitude higher than the rates to Si for wavelengths where the Si optical absorption is indirect. Notice that the $1/d^3$ region begins at

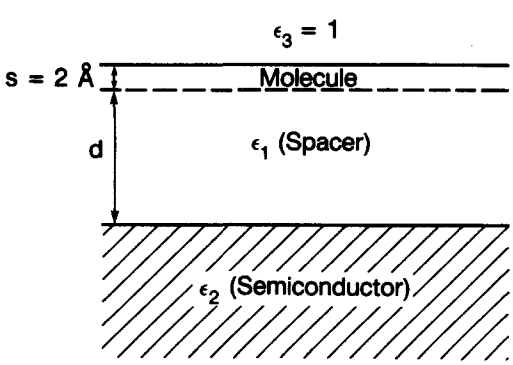

FIG. 1. This is a schematic of the geometry used in the CPS calculations of molecule–semiconductor energy transfer. The ϵ's are the complex optical dielectric constants of the media. The solid lines represent the boundaries between the media, and the dotted line represents the center of the emitting molecule. The molecule–semiconductor separation is d and the molecule–vacuum distance is s.

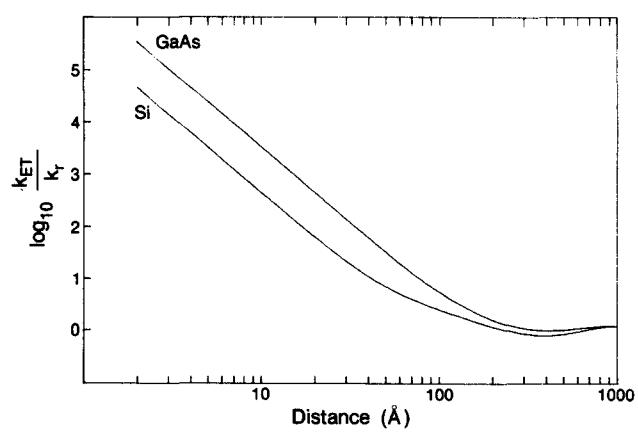

FIG. 2. Log–log plot of the CPS energy transfer rate vs separation from Si and GaAs for a parallel dipole emitting at 3.2 eV with unity quantum yield and radiative rate of 1 s^{-1}.

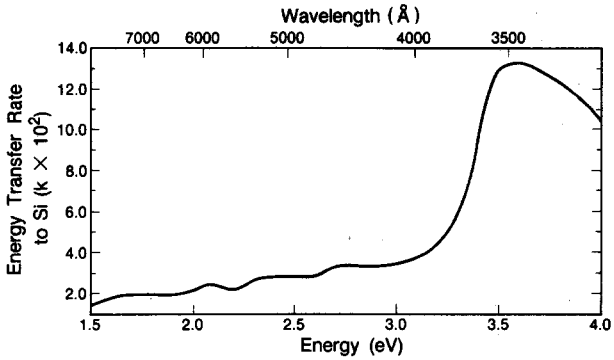

FIG. 3. CPS energy transfer rate vs dipole emission energy for a parallel dipole located 10 Å away from Si. The energy transfer rate increases by an order of magnitude above 3.4 eV, the onset of direct interband absorption.

about 100 Å for GaAs, whereas for Si it occurred at about 50 Å. At small separations, the wavelength dependence is fairly flat throughout the visible for GaAs.

The most important potential limitation of the CPS model is the use of an optical dielectric constant to approximate the response of the solid to the dipole near field. The near field of the molecule contains wave vector components of the order of h/d, where h is Planck's constant and d is the distance from the dipole to the point of observation (compared to h/λ for the radiation field, where λ is the wavelength of the light). Stavola, Dexter, and Knox have discussed the importance of this approximation for molecule–semiconductor energy transfer in a theoretical paper.[5] As an example of what could go wrong, consider that the radiation field can directly excite a vertical transition in the semiconductor band structure, or it can excite a nonvertical transition with phonon assistance. The near field of the molecule, however, can directly excite nonvertical transitions, without phonon assistance, and hence could be more efficient in exciting electrons than the radiation field. This is known schematically for the case of Si in Fig. 4. The approximate distance at which effects of this type could be important is 20 Å, since the wave vector of the dipole near field is a substantial fraction of the semiconductor Brillouin zone at that separation and below.

III. EXPERIMENTAL

A schematic of the experimental apparatus is shown in Fig. 5. Single crystal wafers of Si(111) 500 μm thick, with 10 Ω cm resistivity, were cleaved and etched under inert atmosphere according to the procedure of Aspnes.[38] The samples were mounted on Tantalum backings and placed in a UHV chamber which has been described previously.[39] Tantalum was chosen because, due to its high melting point, it does not interdiffuse with Si at the annealing temperature. The crystals were cleaned by sputtering with 1 kV argon ions at 5×10^{-5} Torr for 1 h, and subsequent annealing for 10 min at 900 °C. Auger spectroscopy showed the crystals to be free of impurities after this treatment.

In a typical experiment the clean Si crystal was cooled to 25 K and the optical constants were monitored in time, using a rotating analyzer ellipsometer, as a spacer layer was grown on the substrate. The change in the optical constants was used to measure the spacer thickness in a manner that has been described previously.[39] A change in Δ of 1.0° corresponded to a 5 Å thick xenon layer, while changes of 0.2° could easily be measured. Once the spacer was deposited, a layer of pyrene could be dosed, using the ellipsometer to monitor the coverage. Zone refined pyrene from Materials by Metron, was introduced into the UHV chamber through a dedicated diffusion pumped inlet line maintained at 150 °C. Once the pyrene was deposited a fluorescence emission spectrum or decay time could be obtained. In a subsequent deposition of pyrene, the ellipsometer could no longer be reliably used to measure the coverage. This is because the errors in measuring, first the optical constants of the bare Si, then the change induced by the Xe spacer, and then the change induced by the pyrene are all compounded. In addition, the ellipsometer readings drift a tenth of a degree over a

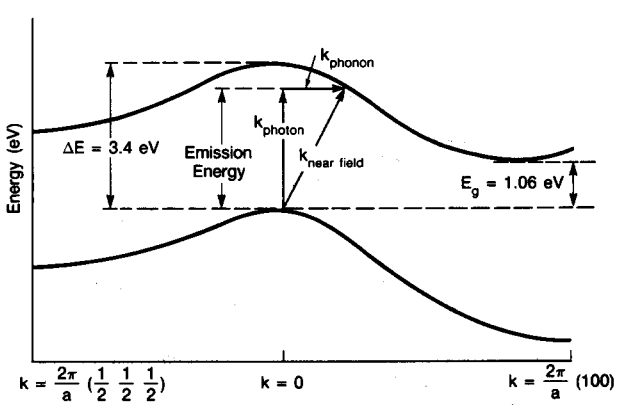

FIG. 4. In this schematic band structure of Si, the molecule–semiconductor energy transfer mechanism is illustrated. Below the onset of direct interband absorption at 3.4 eV, absorption of light requires photon assistance for conservation of momentum. At very short molecule–semiconductor separations, the dipole near field could directly excite a nonvertical interband transition.

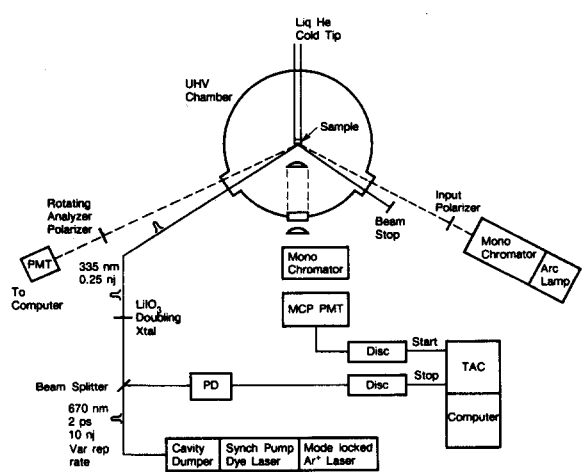

FIG. 5. Schematic of the experimental apparatus. MCP PMT stands for microchannel plate photomultiplier, PD for photodiode, TAC for time to amplitude converter, and Disc for constant fraction discriminator.

period of a few hours, making multiple submonolayer measurements impossible.

Time-correlated single photon counting was employed to measure the lifetimes.[40] The photon counting technique permits the collection of low background decays obeying Poisson statistics with good signal to noise even when the emission is very weak. In addition, this technique has a large dynamic range in time[41,42] (from 50 ps to a few microseconds), and minimizes effects due to laser heating of the substrate. The laser consists of a Coherent CR-8 argon ion laser with the cavity extended to match the Coherent 38 MHz mode-locking frequency. The mode-locked ion laser is used to synchronously pump a Coherent model 700 dye laser, which is also cavity dumped, so that the repetition rate can be adjusted from 3.8 MHz down to single shot. Using DCM, the dye laser produces 40 mW average power at a repetition rate of 3.8 MHz, with a pulse duration of 2 ps. The 670 nm output is doubled in a 1 mm thick $LiIO_3$ crystal, yielding approximately 1 mW of average power at 335 nm.

The peak temperature induced in the sample by this laser can be computed, assuming Gaussian laser pulses in space and in time, and that all the absorbed energy is confined to the surface. Following Brand and George, the temperature rise is given by[43]

$$\Delta T = \frac{49.5(1-R)I(t_p)^{1/2}}{(Kdc\pi)^{1/2}},$$

where R, the reflectance,[29] is 0.563; I, the peak power at the center of the laser beam, is 1 MW/cm^2; t_p, the pulse width in nanoseconds, is 0.002; K, the thermal conductivity,[44] is 10 W/cm K; d, the density is 2.33 g/cm^3; and c, the specific heat[45] is 0.1674 J/g K. Assuming the beam is focused to a 100 μm FWHM spatial pulsewidth, we obtain a peak temperature rise of 0.3 K. The absence of any desorption phenomena upon illumination is supported by the invariance of the fluoresence signal intensity and decay over a period of hours.

In these experiments the fluorescence emission was collected using a quartz lens mounted in the UHV chamber, and the scattered laser light was rejected using an Instruments SA H-10f/3.2 monochromator with a ruled grating with 1200 grooves/mm blazed at 400 nm and 1 mm slits, or 8 nm resolution. The fluorescence was imaged onto the cathode of an RCA C31034A GaAs photomultiplier, or more recently, a Hammamatsu R1564U-01 microchannel plate. The phototube pulses were fed into an EG&G-Ortec model 583 discriminator, the output from which was used as the start pulse for a Canberra 2043 time-to-amplitude converter. A reference pulse from the coherent cavity dumper was used as the stop pulse. A multichannel analyzer was constructed using an ADAC model 1023 100 KHz A/D board interfaced to an LSI 11/73 computer. The instrument response function is about 800 ps using the GaAs phototube and 100 ps using the channel plate.

IV. RESULTS

In these experiments the fluorescence decays from submonolayers of pyrene separated from Si(111) by Xe spacer layers were collected as a function of: (i) coverage; (ii) wavelength; and (iii) separation from Si(111). Time independent fluorescence emission spectra were also collected as a function of coverage. The fluorescence signal was shown to be linear with incident laser intensity, while the fluorescence decays did not change with laser power. Fits of data were performed to the Kohlrausch and to the biexponential decay laws, using the program CURFIT by Bevington,[46] which employs the Marquardt algorithm. The fluorescence decays were sufficiently long that it was unnecessary to deconvolute the instrument response function. A sample fit to a biexponential is shown in Fig. 6(a). Following Richert and Bässler,[32,33] the following form of the Kohlrausch equation was used:

$$J(t) = N(2t)/N(t) = \exp[(1-2^{\alpha})(t/\tau)^{\alpha}] .$$

Fits of the data to this expression requires only two adjustable parameters, and an example of one of the worse fits is shown in Fig. 6(b).

Coverage dependence of the fluorescence emission spectrum as well as the fluorescence decay function was studied

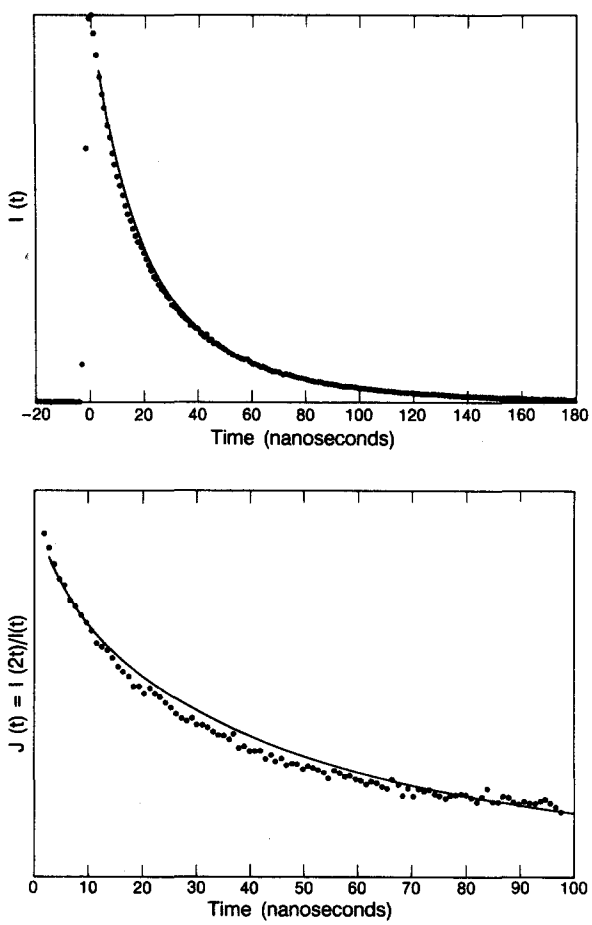

FIG. 6. (a) Fit of a typical fluorescence decay to a biexponential. This decay function was obtained using a 200 Å thick Xe spacer, at a pyrene coverage of approximately two-thirds of a monolayer, and at 390 nm emission wavelength. The points represent the data, the line represents the best fit, with parameters $A_1 = 74.8$, $\tau_1 = 17.2$ ns, $A_2 = 23.6$, $\tau_2 = 54.8$ ns, $\langle\tau\rangle = 36.1$ ns. (b) Fit of the same decay function, to the Kohlrausch form. The fit parameters are $\alpha = 0.636$, $\tau = 15.6$ ns. Note that in performing fits to the Kohlrausch form one adjustable parameter is eliminated by dividing the data at time $2t$ by data at time t.

using a 200 Å thick xenon spacer to separate the pyrene from the xenon. Accurate determination of the coverage for submonolayers has proven difficult in experiments on flat substrates. In this experiment, the coverage dependence could not be reliably determined using the ellipsometer, for reasons which have already been discussed. The best method for determining the trends as a function of coverage was the following. Once the spacer was deposited a small amount of pyrene was deposited while monitoring the fluorescence count level. A fluorescence emission spectrum and a decay function at 390 nm emission wavelength were then collected. More pyrene was deposited, and a new emission spectrum and decay were collected. This process was repeated several times. In this manner there is complete certainty that only the coverage has changed between successive experiments, and that the coverage has increased. Approximate coverage in such an experiment can be inferred by comparison with experiments in which a single deposition of pyrene is performed using the ellipsometer to measure the coverage. Relative fluorescence emission intensity, cannot be used as a measure of coverage, since the quantum yield is presumably changing as a function of coverage along with the fluorescence decay function.

In Fig. 7 are shown the fluorescence emission spectra obtained from an experiment of this type, in which the coverage is varied between approximately one-tenth and one monolayer. At low coverage, there is one band at 390 nm. With increasing coverage this band shifts to lower energy and a new band at 480 nm grows in. The results from fitting the fluoresence decays as a function of coverage are shown in Table II. With increasing coverage, the value of τ and of α, the parameters of the Kohlrausch equation, decrease. The expectation value of the time $\langle\tau\rangle$, derived from the fit to a biexponential, increases with increasing coverage.

The same trends in the wavelength studies were observed at all coverages on the 200 Å thick spacer layers, and the results from one such experiment are shown in Table III. Going from high to low emission energy the relaxation time

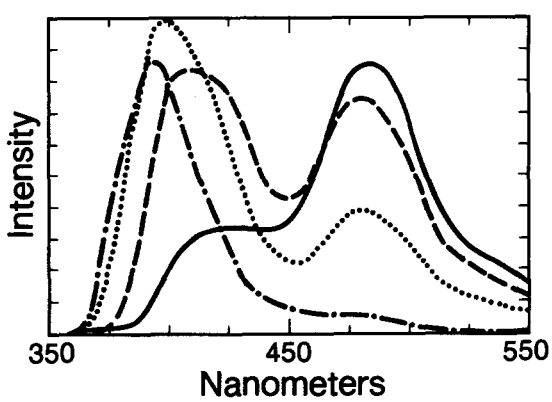

FIG. 7. Fluorescence emission spectra from submonolayer films of pyrene on a 200 Å thick xenon spacer on top of Si(111). The excitation wavelength is 335 nm. At low coverage, there is one peak at 390 nm. With increasing coverage, a peak at 480 nm grows in, while the 390 nm peak shifts. The lowest coverage is estimated to be one-tenth of a monolayer; the highest, one monolayer.

TABLE II. Coverage dependence.[a]

	Kohlrausch equation		Biexponential					
θ	α	τ	A_1	τ_1	A_2	τ_2	$\langle\tau\rangle$	
~0.1	0.927	30.8	68.4	20.8	31.6	42.2	31.1	
	0.812	23.9	65.7	20.9	34.3	42.9	32.3	
	0.837	27.3	61.3		21.5	38.7	43.0	33.5
	0.738	23.0	93.2	28.3	6.8	76.8	36.3	
	0.618	15.3	91.5	26.7	8.5	87.5	40.8	
	0.575	13.6	89.6	26.2	10.4	90.6	44.6	
~1	0.511	12.2		86.1	27.4	13.9	115.	62.6

[a] Shown in this table are the results from a coverage dependence study of the fluorescence decay of pyrene on a 200 Å Xe spacer above Si(111). The decays were collected at 390 nm. The lowest coverage is estimated to be one-tenth of a monolayer, the highest one monolayer. All lifetimes are in nanoseconds.

τ of the Kohlrausch equation, and the expectation value of the time $\langle\tau\rangle$ increased throughout the 390 nm band. The 480 nm band did not show a wavelength dependence.

The distance dependence of the fluorescence decays collected with a 390 nm bandpass interference filter from submonolayers of pyrene on xenon spacer layers of varying thickness is shown in Fig. 8. The coverage was always close to one-half monolayer, as measured ellipsometrically. The appropriate distance is indicated next to each curve. The results of the fits to these decays are shown in Table IV. The lifetime decreases monotonically as a function of molecule–semiconductor separation, for both the double exponential and the Kohlrausch form. The fluorescence signal level which could be obtained with the full repetition rate and unattenuated laser beam was substantially reduced from a few million counts per second at 200 Å to a few thousand at 17 Å.

Fluorescence decays as a function of coverage were collected using 200 Å thick Ar and Kr spacer layers, as well as an 800 Å thick Ar spacer layer. The behavior was qualitatively similar to the Xe spacer layer experiments, but the "rate" of decay was greater on Xe than Kr, and greater on Kr than Ar, presumably due to the external heavy atom effect. Experiments were performed in which cap layers of Xe were grown on top of the pyrene, but the fluorescence decays were unchanged by this procedure.

V. DISCUSSION

In this section, possible mechanisms for the coverage and wavelength dependencies observed on the 200 Å thick spacer layers are discussed. It is concluded that excitation transfer and trapping within the two-dimensional photoexcited overlayer can provide a reasonable explanation for the observations. The decay functions are numerically modeled, and the dependence of the model parameters on coverage and wavelength is physically interpreted. Finally, the question of molecule–semiconductor energy transfer is treated.

While there is a pyrene–spacer layer interaction, it is probably not responsible for the shape of the decay functions, and the observed coverage and wavelength depen-

TABLE III. Wavelength dependence.[a]

	Kohlrausch equation		Biexponential				
λ(nm)	α	τ	A_1	τ_1	A_2	τ_2	$\langle\tau\rangle$
380	0.560	9.35	75.1	15.8	17.2	54.3	32.8
390	0.636	15.6	74.8	17.2	23.6	54.8	36.1
400	0.659	17.8	71.6	18.7	24.8	56.2	37.8
420	0.658	19.2	71.1	19.7	28.7	58.4	40.8
480	0.615	11.5	85.7	17.1	17.7	51.7	30.4

[a] Shown in this table are the results from a wavelength dependence of the fluoresence decay of pyrene on a 200 Å Xe spacer above Si(111). The coverage is estimated to be about two-thirds of a monolayer. All lifetimes are in nanoseconds.

dence. The decays, both in this experiment and in previous molecule–solid energy transfer experiments, are shorter lived for smaller spacer layer thicknesses when the spacers are thin (less than 100 Å), but very similar for thick spacer layers (comparing 200 to 800 Å). Similar results were obtained using Ar, Kr, or Xe as the spacer. For Ar, 25 K is close to the annealing temperature,[36,47] so the Ar spacers should be flat. Matrix spectroscopists have concluded that aromatic hydrocarbons do not diffuse in inert gas matrices unless the temperature is well above the annealing temperature.[47] Amirav and Jortner[48] have studied the fluorescence decays from $(Kr)_n$-tetracene and $(Xe)_n$-tetracene complexes in a molecular beam. They found that the first inert gas atom increased the decay rate of the molecule by an external heavy atom effect, while addition of more inert gas atoms to the complex had no effect. The decays for the Kr complexes remained exponential, while the Xe decays were too fast to observe in time, and could only be studied by comparing relative emission intensities. While none of these observations constitute proof, taken together they suggest that inhomogeneity in the spacers, or spacer–pyrene interaction are not responsible for the dynamics observed here. From the information available, it is not possible to conclude whether the molecules are on top of the spacer layer or partially buried in it, or the details of their arrangement on the surface.

According to the CPS model, at large molecule–semiconductor separations, the radiative rate of the molecule is modulated as a function of wavelength by the reflected field from the semiconductor. The model predicts a wavelength dependence opposite in direction to the one observed for the 390 nm band; no wavelength dependence is observed for the 480 nm band. The radiative rate for the S_1 state of pyrene is on the order of 1 μs, while the decays observed in this experiment are one order of magnitude shorter lived. This suggests that nonradiative processes dominate, and the modulation of the radiative rate by the reflected field from the semiconductor is not important.

It is very plausible that Förster excitation transfer and trapping in the pyrene layer could be responsible for the decays observed. The R_0 for the S_1 state of pyrene in dilute cyclohexane solution is small,[27] only about 10 Å. The exact number for the present configuration cannot be easily obtained since this would require knowing the absorption spectrum of S_1 for the pyrene on the Xe layer. Shifts in the absorption and emission spectra, and changes in the fluorescence quantum yield with coverage, due to associations between ground state pyrene molecules, as observed by Ware for pyrene on silica gel, imply that R_0 depends on coverage as well. At 10% of a monolayer, if the molecules stick wherever they hit the surface, many of the molecules would have nearest neighbors. In addition, it is possible that the molecules can diffuse sufficiently rapidly to form an equilibrium structure.[49] Regardless of whether the distribution is random, or of another type, it appears likely that at

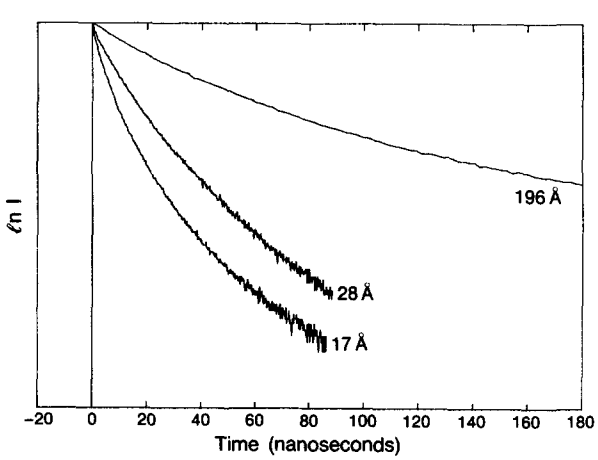

FIG. 8. Fluorescence decay functions for three different spacer layer thicknesses, all collected at 390 nm emission wavelength and at approximately half-monolayer coverage.

TABLE IV. Distance dependence.[a]

	Kohlrausch equation		Biexponential				
d(Å)	α	τ	A_1	τ_1	A_2	τ_2	$\langle\tau\rangle$
196	0.738	23.0	93.3	28.3	6.7	76.8	36.3
28	0.756	8.55	59.0	6.7	32.2	16.3	12.2
17	0.660	3.28	59.3	3.0	29.5	8.7	6.4

[a] Shown here is the distance dependence of the decay function, collected at half-monolayer coverage and at 390 nm emission energy. All lifetimes are in nanoseconds.

10% of a monolayer the pyrene molecules will be close enough for Förster excitation transfer to be important.

It is known from experiments in solution, and the crystalline and amorphous phases, that an electronically excited pyrene molecule can form a complex with a ground state pyrene molecule, and that the resulting excimer is stabilized by a few thousand wave numbers relative to the monomer.[26] At 25 K an excimer cannot dissociate into one excited and one ground state monomer. The monomer emission is located at about 390 nm and the excimer at 480 nm, depending on the environment. The crystal structure of pyrene is dimeric in form, so that almost all the crystal emission takes place from excimers. In the crystal the excimer decay time is temperature dependent, increasing from 115 ns at room temperature to 185 ns at 30 K and below.[50–59] In cyclohexane solution at room temperature the monomer emission lifetime is 445 ns, and the lifetime becomes longer as the temperature is decreased.[26] In the present discussion the assumption will be made that at 25 K the isolated excimer decays faster than an isolated monomer.[61]

The 390 nm emission band observed in the present experiments can be assigned to emission from electronic states localized on one molecule, although these states can be perturbed by the presence of other ground state molecules (e.g., Ware's bound ground state association[22]). The excitation energy can transfer among these "monomer" excited states, and can eventually be trapped by an excimer. Since the intrinsic excimer decay rate is assumed to be faster than the intrinsic monomer decay time, and since the excimers are populated by the monomers, the fluorescence decay function at the excimer emission wavelength will parallel the decay of the monomer population. No rise time need be observed in the excimer emission, since some fraction of the molecules initially excited will be in a position to form an excimer without any hopping. The excimer formation time in the crystal is not yet firmly established, but is certainly much faster than the instrument response in the present experiment.[58,60]

If the spatial and energetic distribution of the molecules on the surface were known, then the exact decay function for the model discussed above could be used to quantify the decays. However, it is very difficult to proceed in the reverse direction, and use the fluorescence decay function alone to determine the appropriate decay law. Decay laws arising from many different physical models, or even from no physical model at all, can produce fits of equal quality from the numerical viewpoint. With a peak count level of 10^4 no more than two nonlinear parameters can reasonably be recovered from the data.[62] The two simplest decay functions in Table I, the Kohlrausch equation and the biexponential, have an acceptably small number of adjustable parameters and produce reasonable fits to the data. By correlating the fitted parameters with the coverage and wavelength dependent studies at a fixed distance, a model for the excitation transfer and trapping can be inferred.

First consider the wavelength dependence of the fluorescence decay function of the disordered submonolayer films. The relaxation time parameter, derived from the fits to either test function, increases within the monomer emission band towards lower energy. The complex fluorescence decays from disordered submonolayer films have previously been modeled by averaging the intralayer hopping time over the spatial distribution of the molecules. It is difficult, however, to explain the wavelength dependence under the assumption that all the molecules are isoenergetic, and that only the spatial distribution is important. This trend is consistent with the spectral diffusion model of Richert and Bässler, in which the site energies are Gaussian distributed with a width that exceeds kT. When the excitation energy jumps from a site higher in energy to one lower, rapid thermalization ensues, so that the reverse process, uphill energy transfer, is much less likely. Excitations higher in energy will tend to diffuse more rapidly, and will tend to find the deep traps, in this case a pair of molecules appropriately oriented for excimer formation, more rapidly than excitations low in the band, and hence the relaxation time will increase towards lower energy. The spatial and energetic distributions are linked, but both must be considered in order to properly understand the dynamics.

As the coverage is increased the amount of excimer emission increases in the fluorescence emission spectrum, so that the concentration of traps, as well as the concentration of monomers, has increased. Seemingly, the decay time ought to decrease with increasing coverage. An examination of the fits to the biexponential form reveals that the expectation value of the time increases with increasing coverage. This paradox can be resolved by examining the fits to the Kohlrausch equation. The parameter α in such a model is inversely related to an inhomogeneous width. The decrease of α with coverage, shown in Table II, from 0.927 to 0.511 as the coverage changes from 0.1 to 1.0 corresponds to a broadening of this width. In the limit of very low coverage an exponential decay will be recovered from the emission of an isolated molecule, while the perturbation due to other molecules on the surface is expected to become more important as the coverage increases, and hence the spectral width should broaden. The shift with coverage in the monomer band observed in the time-independent emission spectra further suggests that the distribution of site energies are coverage dependent.

A physical interpretation for the observed increase in the lifetime with increasing coverage can now be postulated. Because of the energy broadening, the number density of molecules on the surface per unit energy need not increase with total increasing number density. Intuitively this can be understood by comparing a sequence of events in both the high and low coverage cases. At low coverage, the molecules are essentially isoenergetic, allowing the excitation energy to migrate to a trap. At high coverage, the excitation can be "bottlenecked" at a low energy monomer site spatially located far from a deep trap. In such a view, the overall decay can extend to longer times with increasing coverage, in a manner consistent with the coverage dependent fits to the biexponential. The relaxation time parameter from the Kohlrausch equation decreases with increasing coverage because the average distance from an excited monomer to a deep trap has been reduced. The peak of the relaxation time distribution τ shifts to lower values, while the width, which is related to α, becomes larger.

The decays become faster, and the quantum yield drops as the molecule–semiconductor separation is reduced, because of through space energy transfer from the molecule to the semiconductor. This is in agreement with theoretical prediction and previous results on the $^3n\pi^*$ pyrazine/GaAs system, and in contradiction to the results of Hayashi, Castner, and Boyd.[6] This effect will be observed when the molecular emission energy exceeds the semiconductor band gap. The semiconductor should be viewed as a separate, independent trap for the excitation energy. The CPS calculations argue that at 200 Å separation, the intralayer dynamics alone are important; at very short separations, the energy transfer rate to the semiconductor will exceed the hopping rate in the pyrene layer, even at high coverage. Thus at 2 Å, the wavelength dependence of the decay should be dominated by the optical response of the semiconductor, and no coverage dependence to the decay time should be observed. Much of our knowledge concerning molecule–solid energy transfer derives from experiments performed at intermediate separations, between 10 and 100 Å, where both mechanisms will be important. In this regime, the interaction between these mechanisms has not been considered previously. Thus, it will be necessary to perform a coverage and wavelength dependence at more than one molecule–semiconductor separation before these effects can be separated. Should it become possible to experimentally obtain a better measurement of the coverage, the decay time at each molecule–semiconductor separation could be obtained by extrapolation of the relaxation time to 0 coverage.

VI. CONCLUSIONS

In this work it has been demonstrated that when a monolayer of fluorophores is placed near a semiconductor surface both intralayer energy transfer and molecule–semiconductor energy transfer can play an important role in determining the excited state lifetime. A description of the pyrene intralayer dynamics has been borrowed from the field of energy transfer in bulk amorphous solids, and has been applied to the evolution of the dynamics with coverage. This model is distinguished from those which have previously been applied to the problem of energy transfer in disordered submonolayer films, in that an averaging of energy transfer rates is performed over an energetic, rather than a spatial distribution. The notion that the excimers act as traps, and that spectral diffusion take places within the monomer band can qualitatively explain the trends in the 200 Å data, and in particular the wavelength and coverage dependence of the decays. In order to test this description quantitatively, a better experimental determination of the coverage, as well as theoretical work are needed. The CPS calculations and the limited experimental distance dependence which have been presented indicate that image dipole energy transfer plays an important role in determining the lifetimes of molecules near semiconductor surfaces when the molecular emission energy exceeds the semiconductor band gap.

ACKNOWLEDGMENTS

We wish to thank Dr. Michael G. Prisant for useful discussions. This work was supported by the Office of Naval Research. We also acknowledge the U.S. Department of Energy, Office of Basic Energy Sciences, Chemical Sciences Division under Contract No. DE-AC03-76SF00098 for some specialized equipment used in these experiments.

[1] *Laser Chemical Processing of Semiconductor Surfaces*, edited by F. A. Houle, T. F. Deutsch, and R. M. Osgood, Jr. (Material Research Society, Pittsburgh, 1984).
[2] J. H. Fendler, J. Phys. Chem. **89**, 2730 (1985).
[3] P. Anfinrud, R. L. Crackel, and W. S. Struve, J. Phys. Chem. **88**, 5873 (1984).
[4] P. M. Whitmore, A. P. Alivisatos, and C. B. Harris, Phys. Rev. Lett. **50**, 1092 (1983).
[5] M. Stavola, D. L. Dexter, and R. S. Knox, Phys. Rev. B **31**, 2277 (1985).
[6] T. Hayashi, T. G. Castner, and R. W. Boyd, Chem. Phys. Lett. **94**, 461 (1983).
[7] D. H. Waldeck, A. P. Alivisatos, and C. B. Harris, Surf. Sci. **158**, 103 (1985).
[8] N. F. Mott and E. A. Davis, *Electronic Processes in Noncrystalline Solids*, 2nd ed. (Clarendon, Oxford, 1979).
[9] Y. Liang, A. M. Ponte Goncalves, and D. K. Negus, J. Phys. Chem. **87**, 1 (1983).
[10] K. Kenmitz, T. Murao, I. Yamazaki, N. Nakashima, and K. Yoshihara, Chem. Phys. Lett. **101**, 337 (1983).
[11] Y. Liang, P. F. Moy, J. A. Poole, and A. M. Ponte Goncalves, J. Phys. Chem. **88**, 2451 (1984).
[12] F. Willig, A. Blumen, and G. Zumofen, Chem. Phys. Lett. **108**, 222 (1984).
[13] R. L. Crackel and W. S. Struve, Chem. Phys. Lett. **120**, 473 (1985).
[14] D. Oelkrug, M. Radjaipur, and H. Erbse, Z. Phys. Chem. **88**, 23 (1974).
[15] C. H. Lochmüller, A. S. Colburn, M. L. Hunnicut, and J. M. Harris, Anal. Chem. **55**, 1345 (1983).
[16] S. L. Suib and A. Kostapappus, J. Am. Chem. Soc. **106**, 7705 (1984).
[17] C. Francis, J. Lin, and L. A. Singer, Chem. Phys. Lett. **94**, 162 (1983).
[18] K. Chandrasekaran and J. K. Thomas, J. Colloid Int. Sci. **100**, 116 (1984).
[19] G. Beck and J. K. Thomas, Chem. Phys. Lett. **94**, 553 (1983).
[20] K. Chandrasekaran and J. K. Thomas, J. Am. Chem. Soc. **105**, 6383 (1983).
[21] K. Hara, P. de Mayo, W. R. Ware, A. C. Weedson, G. S. K. Wong, and K. C. Wu, Chem. Phys. Lett. **69**, 105 (1980).
[22] R. K. Bauer, P. de Mayo, W. R. Ware, and K. C. Wu, J. Phys. Chem. **86**, 3781 (1982).
[23] U. Even, K. Rademann, J. Jortner, N. Manor, and R. Reisfeld, Phys. Rev. Lett. **52**, 2164 (1984).
[24] D. Rojanski *et al.*, Phys. Rev. Lett. **56**, 2505 (1986).
[25] N. Tamai, T. Yamazaki, I. Yamazaki, and N. Mataga, in *Ultrafast Phenomena V*, edited by G. R. Fleming and A. E. Siegman (Springer, Berlin, 1986).
[26] J. B. Birks, *Photophysics of Aromatic Molecules* (Wiley–Interscience, New York, 1970).
[27] I. B. Berlman, *Energy Transfer Parameters of Aromatic Compounds*, (Academic, New York, 1973).
[28] R. G. Palmer, D. L. Stein, E. Abrahams, and P. W. Andersen, Phys. Rev. Lett. **53**, 958 (1984).
[29] T. Doba, K. U. Ingold, W. Siebrand, and R. A. Wildmann, Chem. Phys. Lett. **115**, 51 (1985).
[30] H. J. Queisser, Phys. Rev. Lett. **54**, 234 (1985).
[31] J. Klafter and A. Blumen, J. Chem. Phys. **80**, 875 (1984).
[32] R. Richert, Chem. Phys. Lett. **108**, 534 (1985).
[33] R. Richert and H. Bässler, J. Chem. Phys. **84**, 3567 (1986).
[34] J. Baumann and M. D. Fayer (to be published).
[35] R. R. Chance, A. Prock, and R. Silbey, in *Advances in Chemical Physics*, edited by S. A. Rice and I. Prigogine (Wiley–Interscience, New York, 1978), Vol. 37, p. 1.
[36] H. E. Hallam and G. F. Scrimshaw, in *Vibrational Spectroscopy of Trapped Species*, edited by H. E. Hallam (Wiley, New York, 1973), p. 45.
[37] D. E. Aspnes and A. A. Studna, Phys. Rev. B **27**, 985 (1983).
[38] D. E. Aspnes and A. A. Studna, Appl. Phys. Lett. **39**, 316 (1981).

[39]P. M. Whitmore, H. J. Robota, and C. B. Harris, J. Chem. Phys. **77**, 1560 (1982).
[40]D. Z. O'Connor and D. Phillips, *Time-correlated Single Photon Counting* (Academic, New York, 1985).
[41]I. Yamazaki, N. Tamai, H. Kume, H. Tsuchiya, and K. Oba, Rev. Sci. Instrum. **56**, 1187 (1985).
[42]M. C. Chang *et al.*, Anal. Instrum. **14**, 433 (1985).
[43]J. L. Brand and S. M. George, Surf. Sci. **167**, 341 (1986).
[44]C. Y. Ho, R. W. Powell, and P. E. Liley, J. Phys. Chem. Ref. Data **3**, Suppl. 1, 587 (1975).
[45]*American Institute of Physics Handbook*, 3rd ed., edited by D. E. Gray (McGraw–Hill, New York, 1972).
[46]P. R. Bevington, *Data Reduction and Error Analysis for the Physical Sciences* (McGraw–Hill, New York, 1969).
[47]B. Meyer, *Low Temperature Spectroscopy* (American Elsevier, New York, 1971), Chap. 6.
[48]A. Amirav, U. Even, and J. Jortner, J. Chem. Phys. **75**, 2489 (1981).
[49]The rate of diffusion of pyrene on a solid Xe surface cannot be easily estimated, as the following crude calculation demonstrates. The Xe–pyrene binding energy can be assumed to be 1000 cm^{-1} (Ref. 48). Following Somorjai [G.A. Somorjai, *Chemistry In Two Dimensions: Surfaces* (Cornell, Ithaca, 1981)], the activation energy for diffusion is assumed to be 200 cm^{-1}; the frequency factor can be obtained by calculating the Boltzmann speed in two dimensions of pyrene at 25 K, which is 1300 cm/s. Assuming a box size of 10, this yields a frequency factor of $1.3\times10^{10}\,s^{-1}$, and a diffusion rate of 0.01 cm/s. If, on the other hand, the activation energy for diffusion were 500 cm^{-1}, the diffusion rate would be slower than 10^{-8} cm/s.
[50]J. B. Birks, A. A. Kazzaz, and T. A. King, Proc. R. Soc. London Ser. A **291**, 557 (1965).
[51]M. Tomura and Y. Takahashi, J. Phys. Soc. Jpn. **31**, 797 (1971).
[52]Y. Takahashi and M. Tomura, J. Phys. Soc. Jpn. **34**, 1014 (1973).
[53]N. Y. C. Chu and D. R. Kearns, Mol. Cryst. Liq. Cryst. **16**, 61 (1972).
[54]K. Uchida and Y. Takahashi, Int. J. Quantum Chem. **18**, 301 (1980).
[55]Y. Takahashi, T. Kitamura, and K. Uchida, J. Lumin. **21**, 425 (1980).
[56]A. Matsui and N. Nishimura, J. Phys. Soc. Jpn. **49**, 657 (1980).
[57]K. Uchida and Y. Takahashi, J. Lumin. **24/25**, 453 (1981).
[58]R. Seyfang, E. Betz, H. Port, W. Schrof, and H. C. Wolf, J. Lumin. **34**, 57 (1985).
[59]A. Inoue, K. Yoshihara, T. Kasuya, and S. Nagakura, Bull. Chem. Soc. Jpn. **45**, 720 (1972).
[60]T. Kobayashi, J. Chem. Phys. **69**, 3570 (1978).
[61]There have been many reports of monomer emission from crystalline or amorphous solid pyrene, in which the monomers are assumed to occupy defect sites (See Refs. 50–60). The lifetimes reported for this type of monomer emission vary from 8 to 900 ns; the observed temperature dependence of the emission has also varied between the experiments, suggesting that the results depend on details of sample preparation.
[62]D. R. James, Y. S. Liu, P. De Mayo, and W. R. Ware, Chem. Phys. Lett. **120**, 460 (1985).